Paleoceanography of the Barents Sea during the Holocene

J.C. Duplessy, E. Cortijo, E. A. Ivanova, T. Khusid, L. Labeyrie, M. Levitan, I. Murdmaa, M. Paterne

Paleoceanography of the Barents Sea during the Holocene

J. C. Duplessy,[1] E. Cortijo,[1] E. Ivanova,[2] T. Khusid,[2] L. Labeyrie,[1] M. Levitan,[2,3] I. Murdmaa,[2] and M. Paterne[1]

Received 17 November 2004; revised 15 April 2005; accepted 20 May 2005; published 7 October 2005.

[1] We measured the oxygen isotopic composition of planktonic and benthic foraminifera in three cores collected at key positions to reconstruct the paleoceanography of the Barents Sea: core ASV 880 on the path of the northern branch of Atlantic water inflowing from the Arctic Ocean, core ASV 1200 in the central basin near the polar front, and core ASV 1157 in the main area of brine formation. Modern seawater $\delta^{18}O$ measurements show that far from the coast, $\delta^{18}O$ variations are linearly linked to the salinity changes associated with sea ice melting. The foraminifer $\delta^{18}O$ records are dated by ^{14}C measurements performed on mollusk shells, and they provide a detailed reconstruction of the paleoceanographic evolution of the Barents Sea during the Holocene. Four main steps were recognized: the terminal phase of the deglaciation with melting of the main glaciers, which were located on the surrounding continent and islands, the short thermal optimum from 7.8 ka B.P. to 6.8 ka B.P., a cold mid-Holocene phase with a large reduction of the inflow of Atlantic water, and the inception of the modern hydrological pattern by 4.7 ka B.P. Brine water formation was active during the whole Holocene. The paleoclimatic evolution of the Barents Sea was driven by both high-latitude summer insolation and the intensity of the Atlantic water inflow.

Citation: Duplessy, J. C., E. Cortijo, E. Ivanova, T. Khusid, L. Labeyrie, M. Levitan, I. Murdmaa, and M. Paterne (2005), Paleoceanography of the Barents Sea during the Holocene, *Paleoceanography*, *20*, PA4004, doi:10.1029/2004PA001116.

1. Introduction

[2] Throughout the last glacial cycle, reorganizations of deep ocean water masses coincided with rapid millennial-scale changes in climate. High- and middle-latitude temperature changes have been less severe during the present interglacial. However, the study of North Atlantic sediment cores revealed a small but continuous sea surface temperature (SST) decrease from the early to the late Holocene [*Marchal et al.*, 2002; *Rimbu et al.*, 2003]. In addition, several ice-rafted events in the northwest Atlantic and the Greenland Sea have been evidenced throughout the Holocene [*Bond et al.*, 1997]. During each of these episodes, cool, ice-bearing waters from north of Iceland were advected to middle latitudes as a result of a substantial change in the North Atlantic's surface circulation [*Bond et al.*, 1997]. However, we still don't know the mechanism of these changes: They could either be linked to thermohaline circulation variations [*Bianchi and McCave*, 1999; *Keigwin*, 1996; *Keigwin and Boyle*, 2000] or constitute a response of the surface ocean to the variability of the atmospheric circulation [*Giraudeau et al.*, 2000; *Rimbu et al.*, 2003].

[3] In order to estimate changes of the flux and characteristics (temperature, salinity) of Atlantic water carried to the high latitudes during the Holocene, we reconstructed the paleoceanography of the Barents Sea. Its only source of warm (~1°C) saline (>35‰) water is an Atlantic water flow carried by the Norwegian-Atlantic Current. This current constitutes the northernmost extension of the ocean conveyor belt. The Barents Sea hydrology is therefore strongly depending on the input of Atlantic water, which is present as a surface water mass in the South West basin in the absence of Arctic water and, more north, as an intermediate water mass separating the Arctic water at the surface from the extremely cold bottom water formed through rejection of brine during freezing [*Midttun*, 1985]. A detailed description of the hydrography of the Barents Sea is given by [*Pfirman et al.*, 1994; *Rudels et al.*, 1994; *Schauer et al.*, 2002].

[4] In this paper, we compared the Holocene isotopic records of oxygen in planktonic and benthic foraminifera from three cores, which allow us to reconstruct the evolution of the major water masses of the Barents Sea during the last 10,000 years. We first compare the $\delta^{18}O$/salinity measurements performed on modern seawater samples collected over recent years. We then interpret the foraminifer $\delta^{18}O$ variations in terms of seawater temperature and $\delta^{18}O$/salinity changes, which both depend on the penetration of Atlantic water into the Nordic seas and the intensity of the thermohaline circulation.

2. Selection of Cores and Local Hydrography

[5] We compared three cores raised from key positions in the Barents Sea (Figure 1). Core ASV 880 (79°55′5 N, 47°08′2 E, 388 m) from the Franz Victoria Trough is on

[1]Laboratoire des Sciences du Climat et de l'Environnement, Laboratoire mixte CNRS-CEA, Gif sur Yvette, France.
[2]Shirshov Institute of Oceanology, Russian Academy of Sciences, Moscow, Russia.
[3]Now at Vernadsky Institute of Geochemistry and Analytical Chemistry, Russian Academy of Sciences, Moscow, Russia.

0883-8305/05/2004PA001116

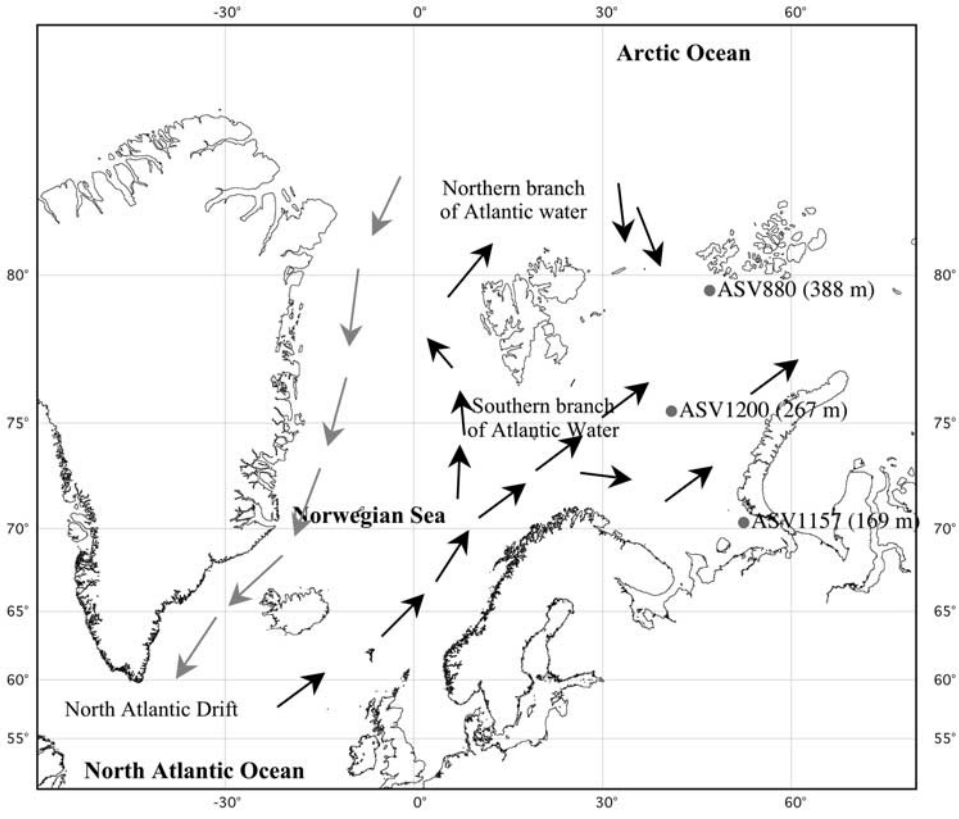

Figure 1. Location of the three cores and main oceanographic currents. The southern branch of Atlantic water (solid arrows) enters into the Barents Sea as a surficial current, whereas the northern branch of Atlantic water (solid arrows) penetrates into the Barents Sea. The shaded arrows indicate the path of the East Greenland Current.

the path of the northern branch of Atlantic water inflowing from the Arctic Ocean. This core was previously studied by *Duplessy et al.* [2001]. Core ASV 1157 (70°32′9 N, 52°47′9 E, 169 m) from the southern margin of Novaya Zemlya is located in a major area of brine formation [*Levitan et al.*, 2003]. In this area, the modified Atlantic water carried by the North Cape and Novaya Zemlya currents was already cooled and mixed with Arctic water to constitute the Barents Sea Water [*Loeng*, 1991]. During winter, surface water salinity is increased by freezing and its density becomes large enough to induce sinking and deep-water formation. Core ASV 1200 (75°44′9 N, 41°00′6 E, 267 m) has been raised from the central Barents Sea. This core is located near the Polar Front, which separates relatively warm and saline water carried by the Norwegian Current from fresher Arctic water in the north.

[6] Temperature and salinity profiles were obtained at the cores' location during summer conditions (Figure 2). They show a low-salinity surficial Arctic water mass (S < 34‰), of which a thin upper layer is heated by the sun: The lower the latitude, the warmer the water. Below 40 m, the Arctic water mixes with the inflowing Atlantic water. This results in a temperature maximum around 100 m water depth, which is well marked at the location of cores ASV 880 and ASV 1200. In the eastern core ASV 1157, close to Novaya Zemlya, winter mixing is so strong that cold (T < −1.8°C), highly saline (S > 35‰) brine water is found below 80 m. This is the water which sinks along bottom slope and flows into hollows and depressions in the sea bottom [*Midttun*, 1985]. At the location of both cores ASV 880 and ASV 1200, the bottom water is composed of a mixture of Atlantic water with the dense water formed through rejection of brine during winter freezing. However, the mixture contains only little Atlantic water at the location of core ASV 1200 and the bottom water is only slightly warmer than the freezing point (T = −1.3°C). The salinity is also smaller (S = 34.91‰) than that of brine water. The percentage of Atlantic water is higher at the location of core ASV 880 than at the location of core ASV 1200. Accordingly, the bottom temperature is higher (T = −0.15°C) than in the central Barents Sea.

3. Modern Sea Water $\delta^{18}O$ Variations

[7] Since the reconstruction of past seawater temperature and salinity rests mainly on the variations of the $\delta^{18}O$ of planktonic and benthic foraminifera in sediment cores, we first studied the oxygen isotopic composition of eastern Barents Sea water in order to relate it to local hydrography. We plotted in Figure 3 the seawater $\delta^{18}O$ versus salinity using data of *Ostlund and Grall* [1993], *Bauch* [1995] and a

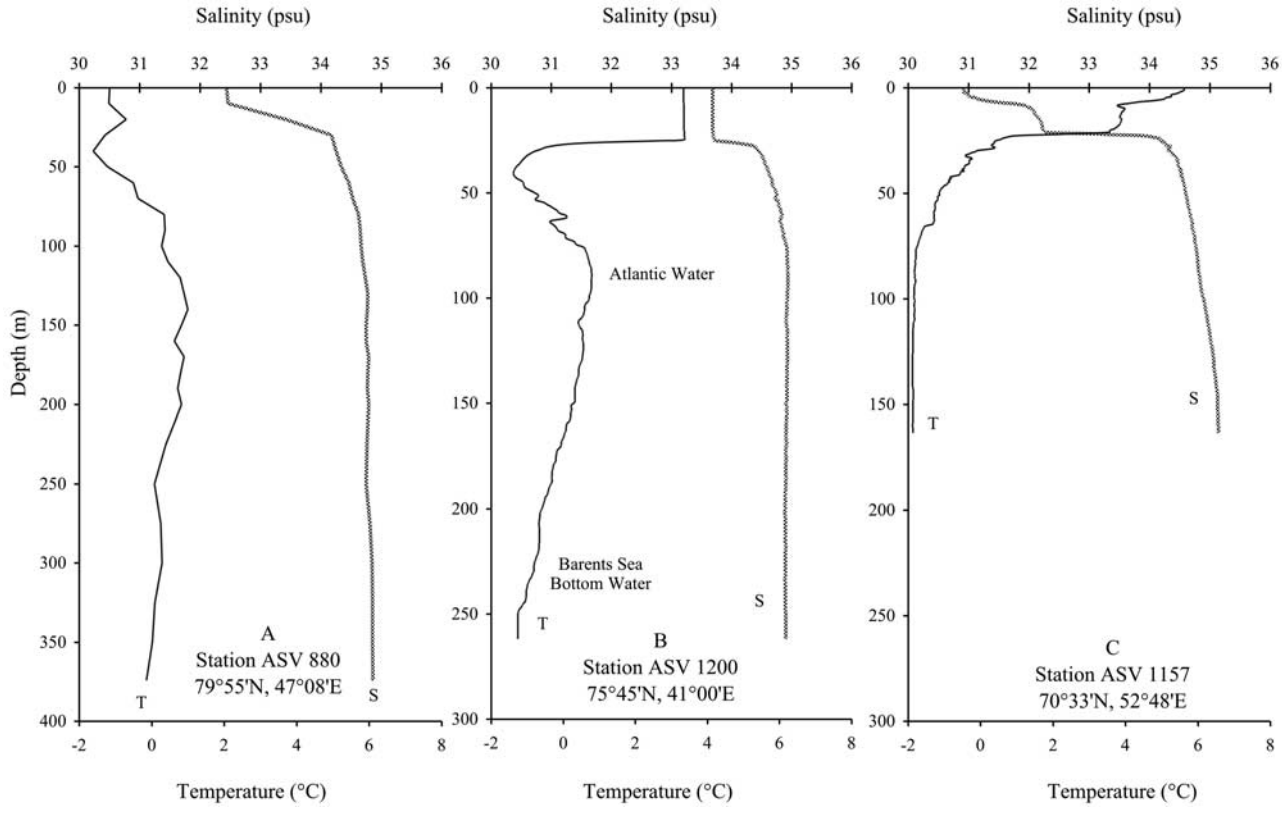

Figure 2. Temperature and salinity profiles at each studied site: (a) ASV 880 on 8 September 1997, (b) ASV 1200 on 13 September 1998, and (c) ASV 1157 on 31 August 1998. (In situ conductivity-temperature-depth measurements were obtained during cruises 11 and 14 of the R/V *Akademik Sergey Vavilov* courtesy of Y. A. Ivanov and V. I. Byshev, Shirshov Institute of Oceanology, Russian Academy of Science).

few open sea data of *Ferronskii* [1978]. Coastal waters influenced by runoff or continental glacier melting exhibit highly scattered values, which depend on the origin of the freshwater. Together with the Atlantic waters, they constitute a broad band, of which the mean freshwater pole has a $\delta^{18}O$ value of $\sim -12.5‰$ (versus SMOW). This value is close to that of the Pechora River outflow ($\delta^{18}O \sim -14‰$) and local precipitation [*Brezgunov et al.*, 1983; *Létolle et al.*, 1993]. In addition, the linear relationship between seawater $\delta^{18}O$ and salinity observed in the case of a mixture of marine and continental water is perturbed here by winter formation of brines and summer sea ice melting, which both modify the salinity without changing significantly the seawater $\delta^{18}O$.

[8] Far from the coast, in the upper 100 m of the water column, seawater $\delta^{18}O$ values exhibit a highly scattered linear trend with salinity. The high-salinity–high-$\delta^{18}O$ values are characteristics of Atlantic water. By extrapolating the $\delta^{18}O$/salinity relationship to pure freshwater, we calculate a $\delta^{18}O$ freshwater value of $\sim -2.75‰$, which is close to the mean $\delta^{18}O$ value of sea ice [*Bauch*, 1995]. Sea ice is formed during winter by freezing of the surficial layer of the Arctic water and melts during summer. The linear trend between salinity and $\delta^{18}O$ shows that mixing between Arctic and Atlantic waters is mainly responsible for $\delta^{18}O$ variations in the upper 100 m of the water column. In the areas of brine formation, the salinity varies between 34.5‰ and 35.2‰ and their $\delta^{18}O$ value is between 0 and +0.40‰.

4. Lithostratigraphy and Radiocarbon Chronology

[9] In all Barents Sea cores, the Holocene constitutes a well-defined unit. It is marked by a characteristic olive gray color (from light to dark olive gray and black because of the presence of hydrotroilite) and replaces the yellowish and brownish shades of Late Glacial sediments. By comparison with glacial deposits, Holocene sediments are also characterized by a dominant clay fraction, a reduced sand fraction, an increased abundance of foraminiferal fauna, and a larger organic matter content [*Ivanova et al.*, 2002; I. O. Murdmaa et al., manuscript in preparation, 2005]. A full description of the cores is given elsewhere [*Murdmaa and Ivanova*, 1999].

[10] The chronology of the cores is based on AMS ^{14}C dates performed on mixed benthic foraminifera or on mollusk shells. Radiocarbon and calendar ages of cores ASV 1157 and ASV 1200 are reported in Table 1. A correction has to be made to take into account the difference between ^{14}C-dated terrestrial plant material and marine shell material (the marine reservoir age). Modern reservoir ages (R) of 320 ± 70 years were measured in mollusk shells as the regional mean and standard deviation (n = 6) for the

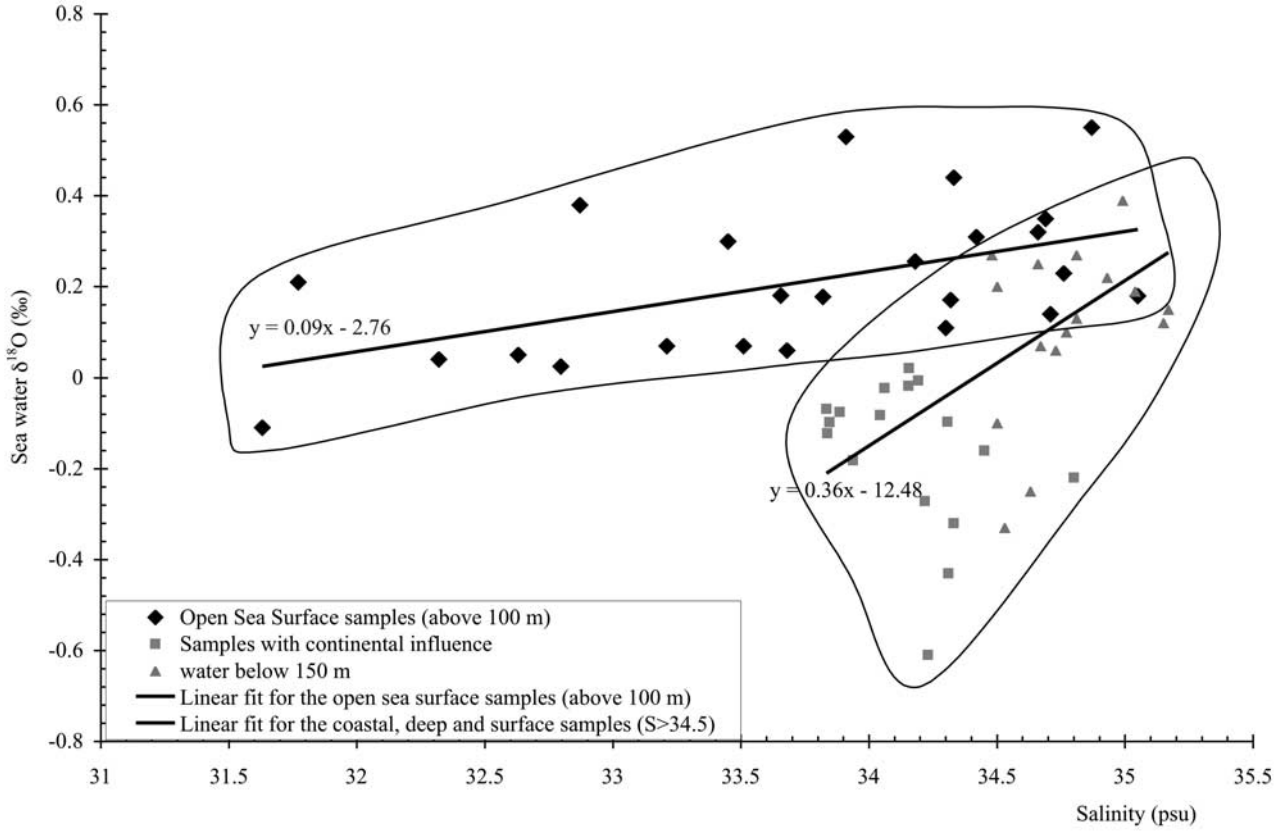

Figure 3. Scatterplot of oxygen isotopic composition of seawater ($\delta^{18}O$ versus standard mean ocean water) versus salinity for the main water masses in the Barents Sea (diamonds, open sea surface samples above 100 m; squares, samples with continental influence; triangles, water below 150 m. The linear regression line ($y = 0.09x - 2.76$) is valid for the open sea surface water samples. The linear regression line ($y = 0.36x - 12.48$) is valid for the other water samples with coastal influence).

coastal Barents Seas [*Forman and Polyak*, 1997], close to the present-day values of R = 410 years in the well mixed open waters of the North Atlantic Ocean [*Bard*, 1988] and of the Norvegian Sea [*Bondevik et al.*, 1999]. Greater reservoir ages of some 640 ± 180 years were not taken into account as they are related to deposit feeder species as *Portlandia artica* [*Forman and Polyak*, 1997]. We therefore applied the 410-year correction, typical for well-ventilated

Table 1. Radiocarbon and Calendar Ages Measured in Cores ASV 1157 [*Levitan et al.*, 2003] and ASV 1200 [*Ivanova et al.*, 2002][a]

Core	Depth, cm	^{14}C age	Error	Age, cal B.P.	Error	Species
ASV1157	13	840	60	472	38	*Macoma calcarea*
ASV1157	50	1900	60	1444	73	*Tridonta borealis*
ASV1157	165	3910	70	3888	82	*Macoma calcarea*
ASV1157	338	6890	90	7392	79	*Leda sp*
ASV1157	355	7290	90	7744	88	*Macoma calcarea*
ASV1157	378	7600	80	8050	95	*Macoma calcarea*
ASV1157	393	8130	90	8606	135	*Macoma calcarea*
ASV1157	398	8160	90	8669	152	*Macoma calcarea*
ASV1157	423	8570	100	9108	177	*Pontlandia artica*
ASV1157	440	8970	90	9483	325	*Macoma calcarea*
ASV1200	7.5	Modern		0		*Yoldiella sp.*
ASV1200	82.5	4660	80	4890	85	*Battyarca sp*
ASV1200	110	5810	70	6225	118	*Yoldiella sp.*
ASV1200	118.5	6200	90	6630	105	*Battyarca sp*
ASV1200	120	6180	60	6610	134	*mix benthics*
ASV1200	195	9220	80	9980	536	*Yoldiella lucida*
ASV1200	205	9450	80	10080	428	*Yoldiella sp.*
ASV1200	210	9550	80	10330	400	*Yoldiella intermedia*
ASV1200	215	9910	90	10735	764	*Yoldiella fraterna*

[a]A 410-year correction has been applied to all conventional ^{14}C ages. ^{14}C ages have been converted into calendar ages using the marine calibration of *Stuiver and Reimer* [1993].

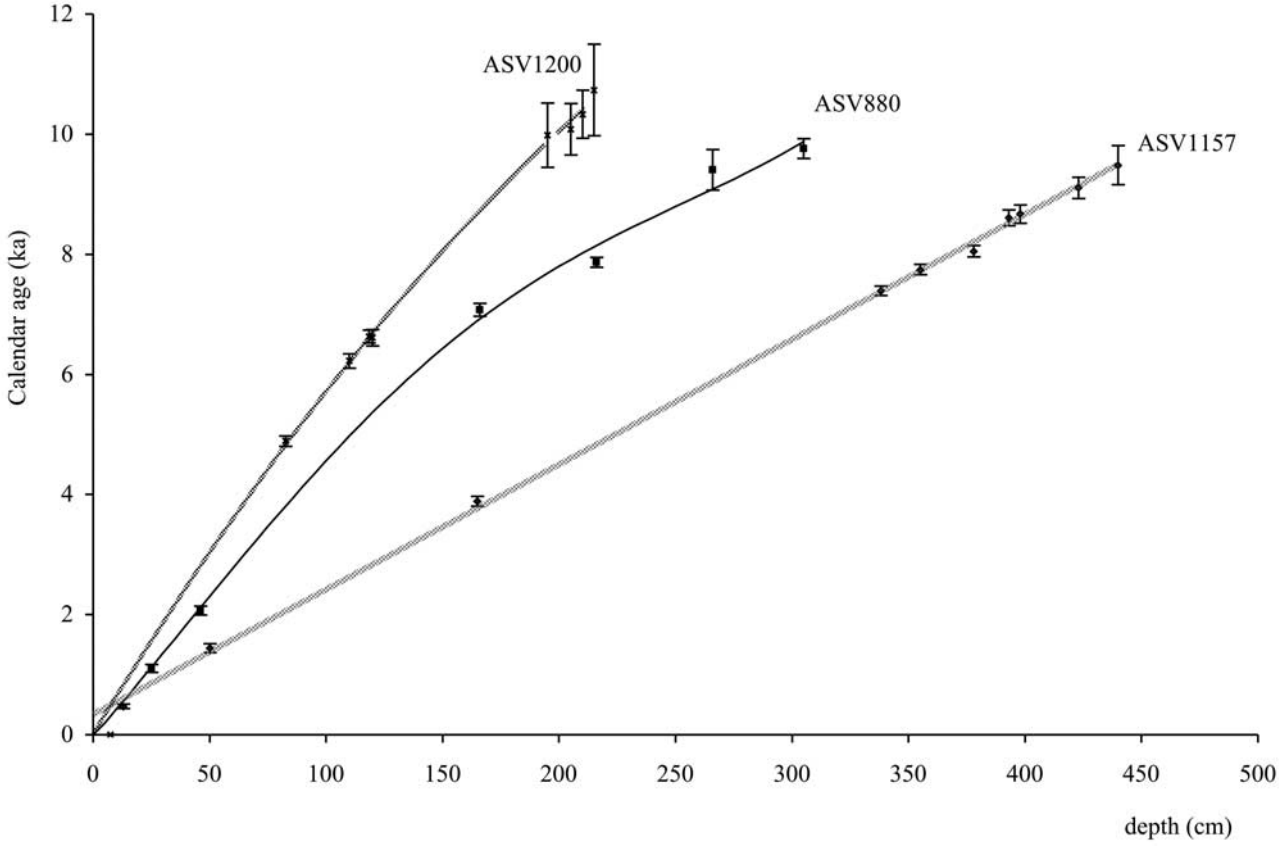

Figure 4. Age-depth relationship for the three cores.

open waters to all conventional ^{14}C ages measured in the Barents Sea cores. ^{14}C ages have then been converted into calendar ages using the marine calibration of *Stuiver and Reimer* [1993], which is well established for the Holocene. The discussion below will therefore refer to calendar ages. The chronology of core ASV 880 has been reported previously [*Duplessy et al.*, 2001]. Figure 4 compares the age-depth relationship in the three Barents Sea cores. Their timescale was generated by computing the best fit between the calendar ages and the core depth: A linear relationship was used for core ASV 1157, a second-order polynomial fit was used for core ASV 1200 and a fourth-order polynomial fit was used for core ASV 880.

5. Foraminifer Oxygen Isotope Records

[11] Stable isotope measurements were performed with a Finnigan MAT 251 mass spectrometer with an automated Kiel Device. The results are presented versus the PDB standard. We used both NBS 19 and NBS 18 as reference standards to ensure a proper calibration on a large range of $\delta^{18}O$ values [*Ostermann and Curry*, 2000]. Oxygen isotopes were measured on the planktonic foraminiferal species *Neogloboquadrina pachyderma* left coiling (lc) in cores ASV 880 and ASV 1200. Core ASV 1157 is totally barren of planktonic foraminifera. *N. pachyderma* lc lives today in the Atlantic water below the Arctic water. Its $\delta^{18}O$ value faithfully records the temperature and $\delta^{18}O$ value of the Barents Sea water at the depth of the temperature maximum, i.e., in the core of the Atlantic water which penetrates into the Barents Sea [*Duplessy et al.*, 2001]. The three cores contain benthic species. The dominant species *Elphidium clavatum* provides a continuous isotope record in both cores ASV 880 and ASV 1200. In core ASV 1157, no benthic foraminifera were found between 5 cm and 195 cm depth. This barren zone, which is observed in numerous cores from the same basin, is not an artifact of the laboratory procedures, because the sediment was kept continuously wet and stored at low temperature (+4°C) before sieving. We believe that the disappearance of foraminiferal shells results from carbonate dissolution at the water sediment interface due to CO_2 production by decaying organic matter [*Levitan et al.*, 2003]. The $\delta^{18}O$ analyses were performed on the most abundant benthic species *Nonion labradoricum*, which is present at the core top and below 195 cm. Results are reported in Table 2.

[12] Figure 5 displays the oxygen isotope records of the three cores. Their general characteristic is the low amplitude of each individual record, which is lower than 1‰. Although not identical, the isotope records of *N. pachyderma* lc exhibit rather similar values in cores ASV 880 and ASV 1200. This similarity reflects the small temperature and salinity difference of Atlantic waters at the location of both cores. By contrast, the benthic record of core ASV 1157 generated with *Nonion labradoricum* exhibits $\delta^{18}O$ values about 0.75 ‰ heavier than those of cores ASV 880 and ASV 1200 generated with *Elphidium clavatum.* This difference cannot be explained only by temperature and salinity differences in the Barents Sea deep waters (see Figure 2).

Table 2. Core Depth, Estimated Ages, $\delta^{18}O$ Versus Peedee Belemnite of Foraminifera, Estimated Global Seawater $\delta^{18}O$ Variations and Local Foraminiferal $\delta^{18}O$ Variations in Cores ASV 880, ASV 1157, and ASV 1200[a]

ASV1200 (*N. pachyderma* sp.)						ASV 1200 (*E. clavatum*)						ASV 1157 (*N. labradoricum*)				
Depth, cm	Polynomial Calendar Age, ka	$\delta^{18}O$ PDB, %	$\delta^{13}C$ PDB, %	Ice Volume Seawater Change	Local $\delta^{18}O$ Variations	Depth, cm	Polynomial Calendar Age, ka	$\delta^{18}O$ + 0.55 PDB, %	$\delta^{13}C$ PDB, %	Ice Volume Seawater Change	Local $\delta^{18}O$ + 0.55 Variations	Depth. cm	Calendar Age, ka	$\delta^{18}O$ − 0.20 PDB, %	$\delta^{13}C$ PDB, %	Ice Volume Seawater Change
0	0.01	3.75	0.35	0.00	3.75	0	0.01	4.51	−1.42	0.00	4.51	0	0.33	4.42	−1.30	0.00
9	0.58	3.68	0.60	−0.01	3.69	2	0.14	4.38	−1.36	0.00	4.38	195	4.40	4.60	−0.40	0.01
19	1.20	3.83	0.49	−0.02	3.85	9	0.58	4.65	−1.32	−0.01	4.66	200	4.50	4.51	−0.60	0.01
21	1.33	3.68	0.49	−0.02	3.70	19	1.20	4.61	−0.96	−0.02	4.62	205	4.60	4.50	−0.49	0.02
39	2.40	3.64	0.54	−0.01	3.64	21	1.33	4.62	−1.46	−0.02	4.63	210	4.71	4.45	−1.00	0.02
44	2.69	3.82	0.62	0.00	3.82	24	1.51	4.53	−1.07	−0.01	4.55	215	4.81	4.63	−0.27	0.02
49	2.98	3.74	0.64	0.01	3.73	29	1.81	4.45	−1.24	−0.01	4.46	220	4.92	4.44	−0.90	0.03
54	3.26	3.71	0.65	0.01	3.70	39	2.40	4.67	−1.16	−0.01	4.68	230	5.12	4.30	−0.30	0.03
59	3.54	3.84	0.83	0.01	3.83	44	2.69	4.65	−1.28	0.00	4.65	235	5.23	4.52	−0.85	0.04
64	3.82	3.67	0.68	0.01	3.66	49	2.98	4.58	−1.31	0.01	4.57	240	5.33	4.44	−1.30	0.04
69	4.10	3.82	0.70	0.01	3.81	54	3.26	4.44	−1.47	0.01	4.43	250	5.54	4.37	−1.20	0.05
79	4.63	3.92	0.67	0.02	3.90	59	3.54	4.54	−1.34	0.01	4.53	260	5.75	4.55	−0.90	0.06
84	4.90	3.49	0.53	0.02	3.46	64	3.82	4.43	−1.68	0.01	4.42	275	6.06	4.44	−1.23	0.07
86	5.00	3.74	0.67	0.03	3.71	69	4.10	4.46	−1.42	0.01	4.45	280	6.17	4.55	−0.90	0.08
89	5.16	3.82	0.64	0.03	3.79	74	4.37	4.33	−1.72	0.01	4.32	290	6.37	4.39	−0.90	0.09
94	5.41	3.56	0.62	0.04	3.52	79	4.63	4.47	−1.27	0.02	4.46	300	6.58	4.37	−0.48	0.10
99	5.67	3.78	0.57	0.05	3.73	81	4.74	4.47	−1.37	0.02	4.45	305	6.69	4.50	−1.30	0.10
101	5.77	3.63	0.52	0.05	3.58	84	4.90	4.54	−1.55	0.02	4.52	310	6.79	4.41	−0.70	0.11
104	5.92	3.79	0.63	0.06	3.73	89	5.16	4.48	−0.98	0.03	4.45	315	6.90	4.45	−0.86	0.11
109	6.16	3.70	0.65	0.07	3.63	94	5.41	4.54	−1.22	0.04	4.50	320	7.00	4.62	−0.66	0.12
119	6.65	3.79	0.65	0.09	3.70	99	5.67	4.51	−1.07	0.05	4.46	325	7.10	4.59	−1.13	0.13
124	6.88	3.75	0.49	0.10	3.65	104	5.92	4.57	−1.66	0.06	4.51	330	7.21	4.67	−1.05	0.13
129	7.12	3.72	0.51	0.12	3.60	109	6.16	4.30	−1.46	0.07	4.23	340	7.42	4.65	−0.91	0.15
149	8.01	3.65	0.30	0.19	3.46	111	6.26	4.59	−1.46	0.07	4.52	345	7.52	4.62	−0.68	0.15
156	8.31	3.81	0.51	0.22	3.59	114	6.41	4.49	−1.22	0.08	4.41	355	7.73	4.77	−0.75	0.16
161	8.53	3.64	0.38	0.24	3.40	119	6.65	4.54	−1.29	0.09	4.45	360	7.83	4.56	−0.67	0.17
184	9.45	3.78	0.12	0.30	3.48	124	6.88	4.60	−1.39	0.10	4.49	370	8.04	4.49	−0.56	0.19
189	9.64	3.70	0.00	0.31	3.39	129	7.12	4.41	−1.29	0.12	4.29	375	8.15	4.62	−1.13	0.20
194	9.83	3.37	−0.10	0.31	3.06	134	7.35	4.58	−1.63	0.13	4.45	380	8.25	4.39	−1.02	0.21
199	10.02	3.81	0.17	0.31	3.51	139	7.57	4.52	−1.64	0.15	4.37	385	8.35	4.08	−1.83	0.22
211	10.45	3.84	0.10	0.32		149	8.01	4.70	−1.21	0.19	4.52	390	8.46	4.54	−1.60	0.23
						151	8.10	4.40	−1.59	0.19	4.21	395	8.56	4.58	−1.40	0.24
						159	8.44	4.60	−1.35	0.23	4.37	400	8.67	4.55	−1.80	0.25
						161	8.53	4.74	−0.99	0.24	4.50	405	8.77	4.41	−1.70	0.26
						164	8.65	4.42	−1.39	0.25	4.17	410	8.87	4.48	−1.19	0.26
						166	8.73	4.46	−1.78	0.26	4.20	415	8.98	4.54	−1.18	0.27
						169	8.86	4.44	−1.48	0.27	4.16	420	9.08	4.39	−1.12	0.28
						171	8.94	4.58	−1.55	0.28	4.30	425	9.19	4.58	−1.92	0.28
						174	9.06	4.57	−1.52	0.28	4.28	430	9.29	4.69	−1.01	0.29
						179	9.26	4.63	−1.15	0.29	4.34	435	9.40	4.20	−2.22	0.29
						184	9.45	4.51	−1.60	0.30	4.21	440	9.50	4.44	−1.65	0.30
						189	9.64	4.55	−1.72	0.31	4.24	470	10.12	4.24	−0.76	0.32
						191	9.72	4.74	−1.46	0.31	4.43					
						194	9.83	4.58	−1.95	0.31	4.27					
						199	10.02	4.64	−1.91	0.31	4.33					
						204	10.20	4.87	−1.66	0.32	4.55					

Table 2. (continued)

ASV1200 (*N. pachyderma* sp.)						ASV 1200 (*E. clavatum*)						ASV 1157 (*N. labradoricum*)					
Depth, cm	Polynomial Calendar Age, ka	$\delta^{18}O$ PDB, ‰	$\delta^{13}C$ PDB, ‰	Ice Volume Seawater Change	Local $\delta^{18}O$ Variations	Depth, cm	Polynomial Calendar Age, ka	$\delta^{18}O + 0.55$ PDB, ‰	$\delta^{13}C$ PDB, ‰	Ice Volume Seawater Change	Local $\delta^{18}O + 0.55$ Variations	Depth, cm	Calendar Age, ka	$\delta^{18}O - 0.20$ PDB, ‰	$\delta^{13}C$ PDB, ‰	Ice Volume Seawater Change	
						209	10.38	4.75	−1.90	0.32	4.43						
						211	10.45	4.74	−1.94	0.32	4.41						
						214	10.55	4.81	−1.54	0.32	4.49						
						234	11.22	4.83	−1.57	0.38	4.45						

[a]Benthic foraminifera $\delta^{18}O$ values have been corrected for disequilibrium (see text).

[13] Benthic foraminifer $\delta^{18}O$ values reflect accurately both temperature and seawater $\delta^{18}O$ values only if the isotopic disequilibrium during calcite precipitation is taken into account [*Duplessy et al.*, 1970, 1984; *Graham et al.*, 1981; *Grossman*, 1984, 1987; *Vincent et al.*, 1981; *Woodruff et al.*, 1980; D. A. R. Poole et al., Stable isotope fractionation in recent benthic foraminifera from the Barents and Kara seas, unpublished manuscript, 1999, hereinafter referred to as Poole et al., unpublished manuscript, 1999]. This isotopic disequilibrium is characteristic of each species. In order to determine it for the species present in Barents Sea sediment, we compared their isotopic composition to that of well-known species, *Melonis barleeanus* and *Cibicides lobatulus*, when these foraminifers were present in the same sediment sample. Results are reported in Table 3. We assume that the correction factor of +0.64‰ for *Cibicides* is also valid for *Cibicides lobatulus.* These measurements show that *Nonion labradoricum* is 0.20 ± 0.15‰ heavier than equilibrium values, whereas *Elphidium clavatum* is 0.55 ± 0.18‰ lighter than equilibrium value. We are confident that this calibration, which may be statistically improved by additional measurements, is basically correct because we determined a correction factor of 0.35 ± 0.18‰ for *Melonis barleeanus,* which is similar to that we apply for this species in the Atlantic Ocean and the Norwegian Sea [*Labeyrie et al.*, 1995, 1987]. It is also in fairly good agreement with the calibration of recent benthic foraminifera from the Barents and Kara seas made by Poole et al. (unpublished manuscript, 1999). We apply this specific correction to all our benthic measurements in order to compare the three benthic records. We also attempt a similar calibration for the $\delta^{13}C$ values of the same species. The very large statistical error of the $\delta^{13}C$ difference between species (Table 3) indicates that different benthic foraminiferal species have different depth habitat in the sediment and that neither *Nonion labradoricum* nor *Elphidium clavatum* $\delta^{13}C$ can be used to reconstruct accurately the $\delta^{13}C$ of the total CO_2 dissolved in the Barents Sea deep water.

[14] After correction for isotopic disequilibrium, foraminifer $\delta^{18}O$ variations reflect both temperature and seawater $\delta^{18}O$ changes. The latter results from three causes whose effects are additive, namely, global continental ice melting and two local causes: changes in the hydrological cycle (precipitation plus runoff plus local glacier melting minus evaporation) and changes in rate of advection and mixing. Global continental ice volume changes were large during the deglaciation and they were still significant during the lower Holocene: The sea level was 33 m below present 10 ka and 20 m below present 7.5 ka [*Bard et al.*, 1990; *Fairbanks*, 1989; *Lambeck and Chappell*, 2001]. The deglaciation was only completed 5.5 ka [*Denton and Hughes*, 1981]. In order to reconstruct foraminifer $\delta^{18}O$ variations due to local seawater temperature and $\delta^{18}O$ changes, we subtracted the seawater $\delta^{18}O$ variations due to global ice sheet melting from the planktonic and benthic $\delta^{18}O$ records of the three cores. We used the seawater $\delta^{18}O$ record computed by *Waelbroeck et al.* [2002]. The resulting local benthic $\delta^{18}O$ records, plotted against calendar age are compared in Figure 6. Similarly, the local $\delta^{18}O$ records of

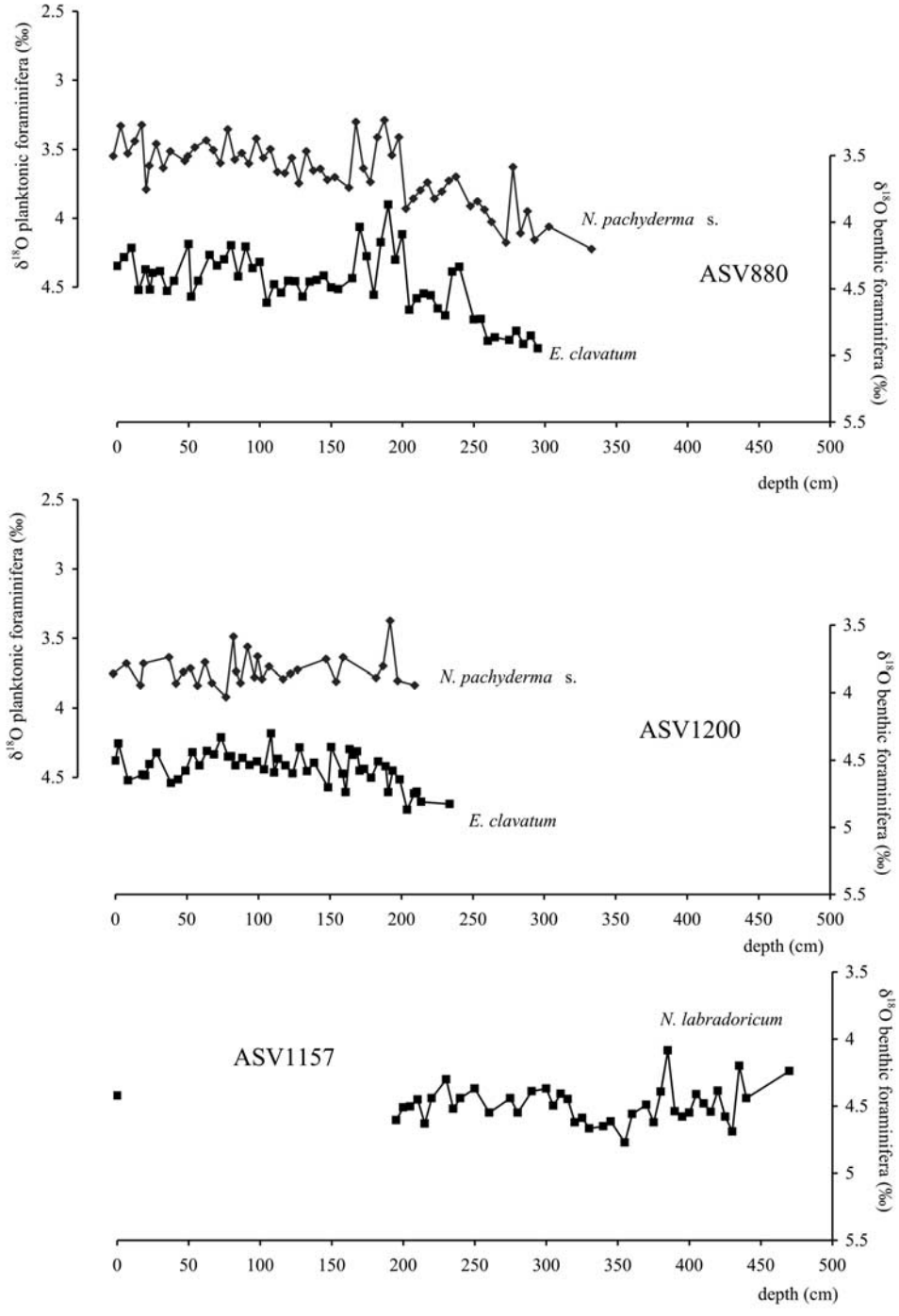

Figure 5. Oxygen isotope ($\delta^{18}O$ versus Peedee belemnite) planktonic and benthic records versus depth for the three cores.

the planktonic species *N. pachyderma* lc in cores ASV 880 and ASV 1200 are reported in Figure 7.

6. Paleoceanographic Evolution of the Barents Sea

[15] The planktonic and benthic isotope records from the three Barents Sea cores exhibit both long-term and high-frequency variations, which permit to distinguish several climatic regimes within the Holocene: The terminal phase of the deglaciation before 7.8 ka B.P. (calendar age before present), a regime with strong Atlantic inflow during the Nordic thermal optimum and during the last 4.7 ka and a regime with weak Atlantic inflow during the middle Holocene.

6.1. Lower Holocene Before 7.8 ka B.P.: Terminal Phase of the Deglaciation

[16] The local $\delta^{18}O$ records of planktonic and benthic foraminifera in the core ASV 880 located in Franz Victoria

Table 3. Synthesis of Comparisons of $\delta^{18}O$ and $\delta^{13}C$ Measurements Performed on Different Foraminiferal Species Found in the Same Sediment Samples of Cores ASV 1157 and ASV 1200[a]

	Foraminifer	Reference	Number of Comparisons	$\delta^{18}O$ Difference	$\delta^{18}O$ Sigma	$\delta^{13}C$ Difference	$\delta^{13}C$ Sigma
ASV 1157	*Elphidium*	*Nonion*	15	−0.84	0.24	−0.69	0.54
ASV 1200	*Elphidium*	*Nonion*	24	−0.74	0.13	−0.19	0.49
ASV 880	*Elphidium*	*Nonion*	40	−0.75	0.13	−0.56	0.42
Mean value				−0.76	0.16	−0.47	0.5
ASV 1183	*Elphidium*	*Cibicides*	5	0.35	0.15	−2.53	0.42
ASV 1200	*Elphidium*	*Cibicides*	29	0.08	0.15	−2.6	0.36
ASV 880	*Elphidium*	*Cibicides*	17	0.02	0.17	−2.86	0.32
Mean value				0.09	0.18	−2.68	0.37
ASV 1183	*Melonis*	*Cibicides*	31	0.29	0.18	−2.45	0.2
ASV 1200	*Nonion*	*Cibicides*	18	0.83	0.15	−2.41	0.51

[a]Digital values for core ASV 880 were previously published by *Duplessy et al.* [2001].

Trough at the northern limit of Barents Sea exhibit some light $\delta^{18}O$ peaks, but no major long-term trends. By contrast, the local records of planktonic and benthic foraminifera in cores ASV 1157 and ASV 1200 located more south exhibit an increasing trend, with $\delta^{18}O$ values still lower or equal to those of core ASV 880 (Figures 6 and 7). In addition, both records exhibit light $\delta^{18}O$ peaks. As we have no additional proxy to estimate sea surface temperature (SST) independently from isotope measurements, two hypotheses could explain these low $\delta^{18}O$ values: First, they may reflect warmer SST in the southern and middle Barents Sea. At this time, the Norwegian Current and the West Spitzbergen Current were warmer than today [*Hald and Aspeli*, 1997; *Hald et al.*, 2003, 2004; *Sarnthein et al.*, 2003] so that the inflow of warm Atlantic water might have resulted in high SST in the central, eastern and northern Barents Sea. However, whereas the warming appears continuous during the lower Holocene in the western Barents Sea, the isotope records in Figures 6 and 7 exhibit only light $\delta^{18}O$ peaks of short duration. The climate records of the western and eastern basins of the Barents Sea are not fully comparable.

[17] An alternative hypothesis would interpret these light $\delta^{18}O$ values as deriving from local freshwater input resulting from melting of nearby glaciers. Although most of the deglaciation of the eastern Barents Sea was already achieved by the beginning of the Holocene [*Forman et al.*, 1996], evidence for continuing deglaciation and ice

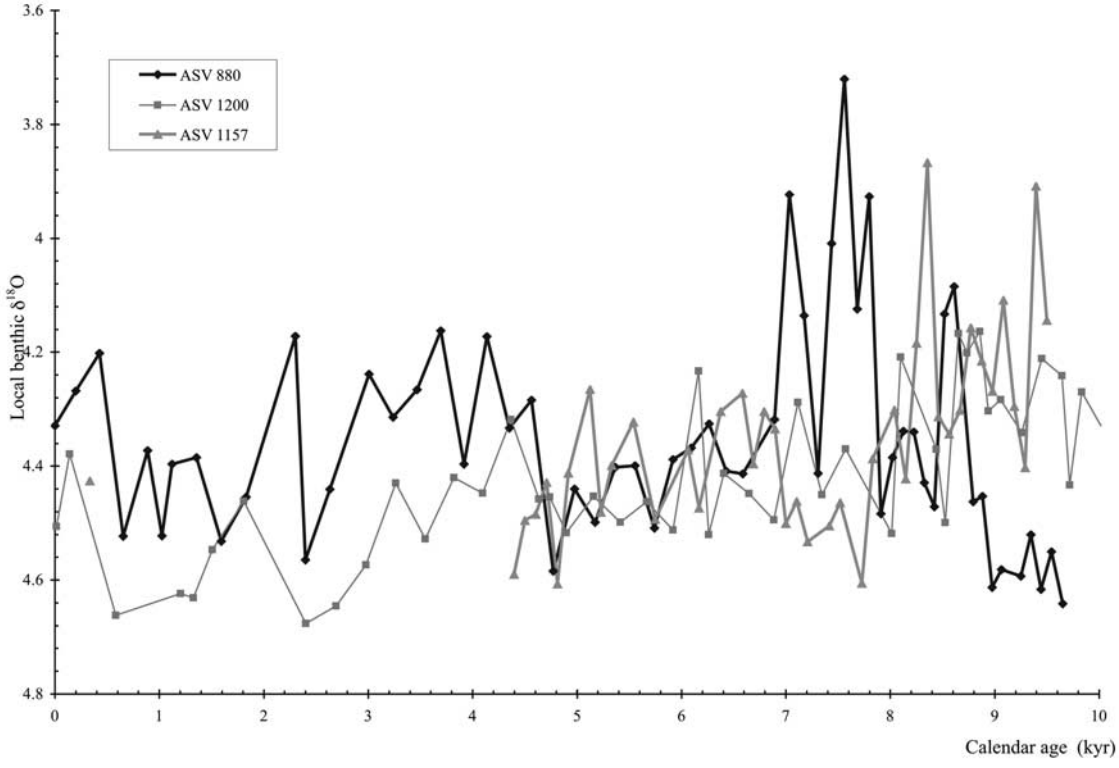

Figure 6. Local oxygen isotope records for benthic foraminifers in cores ASV 880, ASV 1157, and ASV 1200. See color version of this figure at back of this issue.

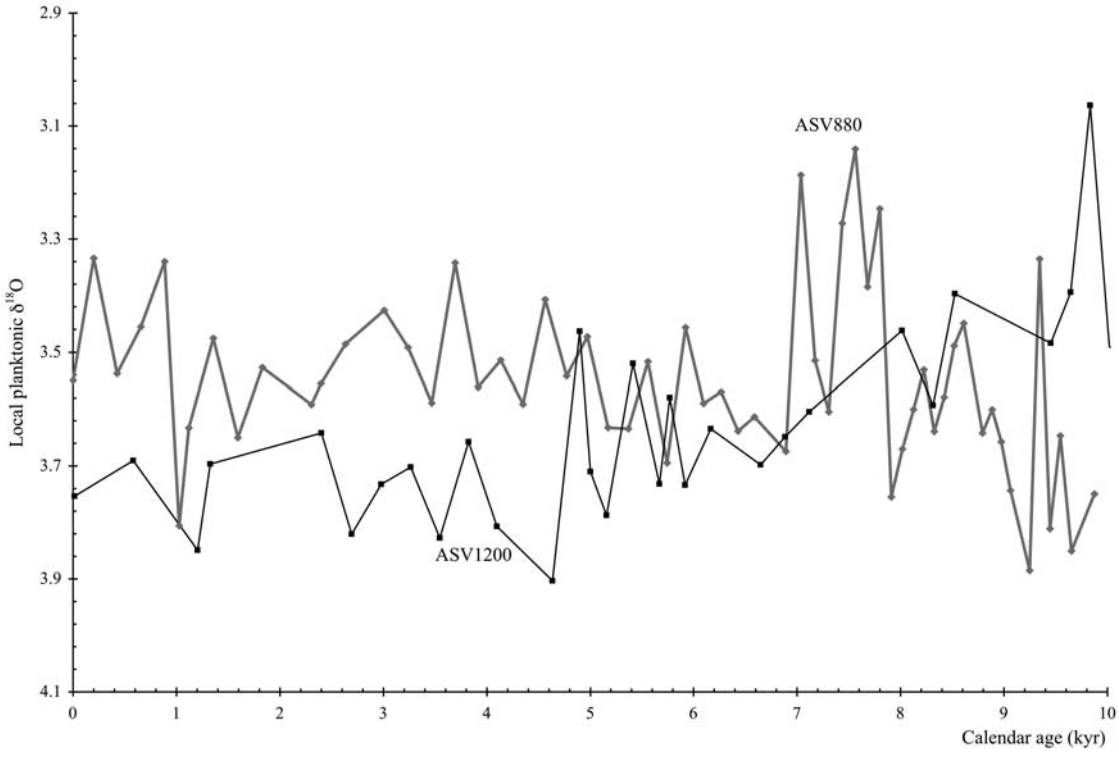

Figure 7. Local oxygen isotope records for planktonic foraminifers in both cores ASV880 and ASV1200.

rafted transport is provided by coarser sediments before 8 ± 0.2 kyr B.P. in cores ASV 880 and ASV 1157 and glaciomarine deposits in core ASV 1200 [*Murdmaa and Ivanova*, 1999]. As a consequence, local seawater $\delta^{18}O$ variations might have a measurable impact on the foraminiferal $\delta^{18}O$ record. *Lubinski et al.* [2001] also showed that during the deglaciation, planktonic and benthic foraminifera from Barents Sea cores exhibited $\delta^{18}O$ values even lower than present, coincident with glacial marine sediment deposition. The $\delta^{18}O$ variations of core ASV 1157 and ASV 1200 at the beginning of the Holocene might therefore represent a record of the terminal deglaciation phase of islands and continental lands surrounding the Barents Sea. As this signal is predominantly found in cores ASV 1157 and ASV 1200, we assume that the input of meltwater originated mainly from land-ice masses located in the southern side of the Barents Sea, i.e., Novaya Zemlya and the European continent. Around 8.5 ka B.P., the three cores exhibit a sharp $\delta^{18}O$ light peak. These peaks are synchronous within the uncertainties of ^{14}C dating. They may reflect either a warm event observed at the scale of the whole Barents Sea or the last large meltwater event recorded in this basin.

6.2. A Strong Atlantic Inflow During the Thermal Optimum and the Last 4.7 ka

[18] Between 7.8 and 6.8 ka B.P. and during the last 4.7 ka, the planktonic and benthic $\delta^{18}O$ records show that the water column below the Arctic water at the location of core ASV 880 was significantly warmer than in the central Barents Sea. This hydrologic pattern, qualitatively similar to the present is the signature of a large inflow of Atlantic water into the Barents Sea.

[19] Between 7.8 and 6.8 ka B.P., the local $\delta^{18}O$ record of the planktonic species *N. pachyderma* lc in core ASV 880 exhibits a well-marked double $\delta^{18}O$ light peak. Its large amplitude, which is close to 0.5‰ most likely indicates that the Atlantic water flowing from the Arctic Ocean to the Barents Sea as an intermediate water mass in the Franz Victoria Trough was warmer than 2°C. This feature marks the Holocene thermal optimum in the Barents Sea and compares nicely to a similar warming measured in the $\delta^{18}O$ record of *N. pachyderma* lc in a core raised from the St Anna Trough [*Hald et al.*, 1999]. As a similar $\delta^{18}O$ light peak is observed in the benthic record of the same core, the whole deep water column below the Arctic water was therefore warmer than today, indicating an Atlantic inflow larger than the modern. In core ASV 1200, *N. pachyderma* lc is extremely rare and only one level was rich enough for isotope analysis (Figures 5 and 7). No conclusion on the flux of Atlantic water brought into the southern Barents Sea by the North Cape Current during this thermal optimum can be drawn from one single analysis, which however indicates the presence of cold water in the central Barents Sea.

[20] The isotopically light double $\delta^{18}O$ peak found in the benthic record of core ASV 880 coincides with a $\delta^{18}O$ increase of ~0.2‰ in the benthic record of core ASV 1157, leading to slightly higher than modern values (Figure 6). As this latter core has been raised from an area of major brine formation under modern conditions, the bottom temperature

cannot have been lower than today in the past. The +0.2‰ $\delta^{18}O$ increase measured in the benthic record of core ASV 1157 indicates first that the bottom water was not warmer than today during the Holocene thermal optimum. Second, it shows that the bottom water $\delta^{18}O$ at the core location was 0.2‰ heavier than modern values. Surface water sinking occurs without change in its $\delta^{18}O$ value. The $\delta^{18}O$ increase of ~0.2‰ in the benthic record of core ASV 1157 indicates therefore that the surface water, which sank during winter, was also 0.2‰ heavier than modern value. Under modern conditions, brine water $\delta^{18}O$ values are 0.3 to 0.4‰ lower than Atlantic waters because of their dilution by freshwater [*Bauch*, 1995]. Our measurements indicate that during the Holocene thermal optimum, the dilution of Atlantic water by fresh, $\delta^{18}O$-light Arctic water was reduced by about 50% as compared to today and that the mechanism of Barents Sea bottom water formation by brine sinking was still active. We stress that these data, which provide a characterization of the composition of the mixture constituting the brine water, provide no information on the flux of the brine and their variations during the Holocene.

[21] Assuming that the brine water temperature was close to the freezing point, the $\delta^{18}O$ difference between cores ASV 880 and ASV 1157 would indicate that the deep water in Franz Victoria Trough was, like the Atlantic water at intermediate depth, warmer than today by ~2°C during the thermal optimum. The mixture of Atlantic water with brine water which constituted the deep water mass at the location of core ASV 880 therefore contained less brine water than today, so that the stratification was minimal [*Duplessy et al.*, 2001]. We note that this optimum was interrupted by a strong cooling of short duration, which is also observed in the planktonic record of core ASV 880.

[22] The benthic record of core ASV 1200 exhibits $\delta^{18}O$ values slightly lighter than those of core ASV 1157. These values are intermediate between those measured in cores ASV 1157 and ASV 880. They show that the deep water in the central Barents Sea was like today a mixture of Atlantic water and Barents Sea bottom water, with a low temperature, about 0.5 to 1°C above the freezing point.

6.3. A Reduced Penetration of Atlantic Water During the Mid-Holocene

[23] Between 6.8 and 4.7 ka B.P., the three cores display almost identical benthic $\delta^{18}O$ values, which are similar to present-day values at the location of core ASV 1157. The Barents Sea deep water below 250 m was therefore uniformly cold, with a temperature close to the freezing point, similar to that of the deep water in the formation area near Novaya Zemlya. This suggests that the Barents Sea deep water, which is a mixture of Atlantic water with brine water was dominated by brine water near the freezing point and that the Atlantic flow brought to the Nordic Seas was much smaller than during the thermal optimum.

[24] The reduced inflow of Atlantic water resulted in a significant cooling of the water mass around 100 m depth in Franz Victoria Trough. This is marked by a sharp increase in the $\delta^{18}O$ records of *N. pachyderma* lc of core ASV 880. The Atlantic water penetrating into the Barents Sea from the north was about 0.5°C colder than today in the Franz Victoria Trough. These features point to a sharp reduction of the heat transport into the Barents Sea by the Norwegian-Atlantic current, which flows northward along the coast of Norway. A progressive warming at a mean rate of 0.25°C/ka led to the modern conditions by 4.7 ka B.P.

7. Discussion

[25] An early Holocene temperature maximum has already been found in both continental and marine records of the high latitudes of the Northern Hemisphere. Evidence was reviewed by *Crowley and North* [1991] and *Duplessy et al.* [2001]. This warming is probably due to the penetration of temperate Atlantic water into the Nordic seas. It is recorded as early as 11.8 kyr B.P. in the subarctic Fjord Malanger, northern Norway [*Hald et al.*, 2003] and 10.8 kyr B.P. in the northern Norwegian Sea at 75°N [*Sarnthein et al.*, 2003]. By contrast with the climatic evolution of the Norwegian Sea and most of the European continent, the thermal optimum has a very short duration in the Barents Sea (about 1000 years). More south, near 67°N, a detailed paleoclimatic record from the eastern Vöring Plateau shows that the period of maximum warmth lasted for 3000 years [*Birks and Koç*, 2002]. It began at about 9700 yr B.P., i.e., 2000 years before the thermal optimum of the Barents Sea (our cores and those of *Hald et al.* [1999]) and finished about 6700 years B.P., almost simultaneously with the end of the warm episode in the Barents Sea.

[26] The thermal optimum in the Nordic seas appeared about 2 ka at 67°N and 4 ka at 80°N after the June solar insolation maximum at 70°N. The lag in temperature versus insolation indicates that, in addition to insolation, local feedback mechanisms, such as the slow melting of the remnants of the continental ice sheets or sea ice variations played a significant role in the regional climate and delayed the warming at 80°N with respect to that of lower latitudes.

[27] The mid-Holocene cooling observed in the Barents Sea is also recorded at lower latitude on the Vöring Plateau, where a SST reconstruction exhibits also a gentle cooling trend between 6.7 and 4.7 ka B.P. [*Birks and Koç*, 2002] and in the northern Norwegian Sea, where it began around 7.8 kyr B.P., culminated at 6.8 kyr B.P. and then experienced minor fluctuations until 2 kyr B.P. [*Sarnthein et al.*, 2003]. This slow temperature decrease contrasts sharply with the abrupt cooling of the water column at intermediate depth and near the bottom observed in the northern Barents Sea around 6.8 ka. The diatom record of *Birks and Koç* [2002] also shows that at the same time, the assemblage associated with the North Atlantic water decreased, whereas that of Norwegian-Atlantic water began to increase continuously for 2000 years. This trend is similar to the small warming depicted by the $\delta^{18}O$/temperature records of *N. pachyderma* in both Barents Sea cores ASV 880 and ASV 1200. This observation suggests that the broad intense warm Atlantic current, which fed directly the Nordic seas during the thermal optimum [*Koç et al.*, 1993], was suddenly

reduced by 6.7 ka and did not reach any more the Barents Sea. This reduction in direct Atlantic flow was compensated by a strengthening of the Norwegian-Atlantic current carrying Atlantic water mixed with coastal waters along the coast of Norway. In the northern Barents Sea, the temperature variations of the Atlantic water mass at a depth around 100 m recorded first the disappearance of the direct Atlantic flow as a sharp cooling and the increasing intensity of the Norwegian Current by a small warming trend leading to temperatures close to the present.

[28] The setting of the modern regime in the Barents Sea coincides with a change in the diatom assemblage on Voring Plateau and a small temperature decrease during summer [*Birks and Koç*, 2002]. This regime persisted up to now with minor oscillations of the temperature of both the deep and intermediate water masses water in Franz Victoria Trough and central Barents Sea. Modern ship observations show that the transport of Atlantic water to the Barents Sea depends mainly on the wind field associated with the North Atlantic Oscillation. During the positive phase of the North Atlantic Oscillation, strong westerlies result in a larger and warmer flux of Atlantic water transported both by the North Cape Current directly to the Barents Sea and by the current which enters the Arctic Ocean through Fram Strait [*Dickson et al.*, 2000] and continues at intermediate depth. Our data point to long-term (centennial to millennial) fluctuations of both the flux of Atlantic water penetrating into this basin and the temperature of the water column in the northern and central Barents Sea. Since the Holocene thermal optimum and the disappearance of the broad Atlantic flow which directly fed the Nordic seas, the fluctuations of the westerlies intensity appear as a potential cause for the variations of the Barents Sea hydrology during the last 6.8 ka. This mechanism, which has been already invoked to explain instabilities in surface circulation south of Iceland [*Giraudeau et al.*, 2000] and in sea surface temperature in the North Atlantic [*Rimbu et al.*, 2003] and in the eastern Norwegian Sea during Holocene times [*Risebrobakken et al.*, 2003] might well be the dominant factor driving the North Atlantic circulation, not only on decadal but also on centennial to millennial timescales since 4.7 ka.

8. Conclusion

[29] The paleoceanographic evolution of the Barents Sea during the Holocene is characterized by four main steps: the terminal phase of the deglaciation with melting of the main glaciers,, which were located on the surrounding continent and islands, the short thermal optimum from 7.8 ka B.P. to 6.8 ka B.P., a cold mid-Holocene phase with a large reduction of the inflow of Atlantic water and the inception of the modern hydrological pattern by 4.7 ka B.P.

[30] Both global and local factors were responsible for the evolution of the hydrology and climate of the Barents Sea. The deglaciation and the subsequent warming were triggered by the increase of the high-latitude insolation, but local glacier melting maintained cold and low-salinity surface waters up to 7.8 ka B.P., whereas the Norwegian Sea experienced warm conditions since about 10 ka B.P. The end of the thermal optimum was synchronous in both basins as a consequence of a sharp reduction of warm Atlantic water to the Nordic seas. This flow increased again after 4.7 ka B.P. and modern conditions were established at that time. Minor fluctuations of the surface and deep water temperature of the Barents Sea may be related to centennial to millennial-scale variations of the intensity of westerlies in the North Atlantic.

[31] **Acknowledgments.** We thank D. Bauch and M. Hald for providing modern seawater salinity and $\delta^{18}O$ measurements together with useful comments on the modern hydrography of the Barents Sea. The sediment cores were collected during cruises by R/V *Akademik Sergei Vavilov* financed by P. P. Shirshov Institute of Oceanology, Russian Academy of Sciences. We acknowledge RFBR-CNRS (PICS grant 98-05-22029), CEA, CNRS-INSU (IMPAIRS), and EU-DGXII (ENVC-CT97-0643) for financial support. We thank E. Jansen and J. C. Gascard for useful discussions. We are grateful to N. Bubenchikova for assistance with foraminiferal sampling; to B. Le Coat, E. Kaltnecker, and N. Tisnerat for isotope analyses; to Y. A. Ivanov and V. I. Byshev for hydrological data; and L. V. Polyak for taxonomic help.

References

Bard, E. (1988), Correction of accelerator mass spectrometry ^{14}C ages measured in planktonic foraminifera: Paleoceanographic implications, *Paleoceanography*, *3*, 635–645.

Bard, E., B. Hamelin, and R. G. Fairbank (1990), U-Th ages obtained by mass spectrometry in corals from Barbados: Sea level during the past 130000 years, *Nature*, *346*, 456–458.

Bauch, D. (1995), The distribution of $\delta^{18}O$ in the Arctic Ocean: Implications for the freshwater balance in the Halocline and the sources of deep and bottom waters, *Rep. 159*, 144 pp., Alfred Wegener Inst., Bremerhaven, Germany.

Bianchi, G. G., and I. N. McCave (1999), Holocene periodicity in North Atlantic climate and deep-ocean flow south of Iceland, *Nature*, *397*, 515–517.

Birks, C. J. A., and N. Koç (2002), A high-resolution diatom record of late-Quaternary sea-surface temperatures and oceanographic conditions from the eastern Norwegian Sea, *Boreas*, *31*, 323–344.

Bond, G., W. Showers, M. Cheseby, R. Lotti, P. Almasi, P. deMenocal, P. Priore, H. Cullen, I. Hajdas, and G. Bonani (1997), A pervasive millennial-scale cycle in North Atlantic Holocene and glacial climates, *Science*, *278*, 1257–1266.

Bondevik, S., H. H. Birks, S. Gulliksen, and J. Mangerud (1999), Late Weichselian marine ^{14}C reservoir ages at the western coast of Norway, *Quat. Res.*, *52*, 104–114.

Brezgunov, V. S., V. Debolskii, V. V. Nechaev, V. I. Ferronskii, and T. V. Yakimova (1983), Characteristics of the formation of the oxygen isotopic composition and salinity upon mixing of sea and river waters in the Barents and Kara seas, *Water Resour.*, *9*, Engl. Transl., 335–344.

Crowley, T., and G. North (1991), *Paleoclimatology*, Oxford Univ. Press, New York.

Denton, G., and T. Hughes (1981), *The Last Great Ice Sheets*, John Wiley, Hoboken, N. J.

Dickson, R. R., T. J. Osborn, J. W. Hurrell, J. Meincke, J. Blindheim, B. Aslandvisk, T. Vinje, G. Alekseev, and W. Maslowski (2000), The Arctic Ocean response to the North Atlantic Oscillation, *J. Clim.*, *13*, 2671–2696.

Duplessy, J. C., C. Lalou, and A. C. Vinot (1970), Differential isotopic fractionation in benthic foraminifera and paleotemperatures reassessed, *Science*, *168*, 250–251.

Duplessy, J. C., N. J. Shackleton, R. K. Matthews, W. Prell, W. F. Ruddiman, M. Caralp, and C. H. Hendy (1984), ^{13}C record benthic foraminifera in the last interglacial ocean: Implications for the carbon cycle and the global deep water circulation, *Quat. Res.*, *21*, 225–243.

Duplessy, J. C., E. Ivanova, I. Murdmaa, M. Paterne, and L. Labeyrie (2001), Holocene paleoceanography of the northern Barents Sea and variations of the northward heat transport by the Atlantic Ocean, *Boreas*, *30*, 2–16.

Fairbanks, R. G. (1989), A 17000-year glacio-eustatic sea level record: Influence of glacial melting rates on the Younger Dryas event and deep-ocean circulation, *Nature*, *342*, 637–642.

Ferronskii, V. I. (1978), Investigation of the distribution of oxygen-18 and tritium in waters of the Barents and Kara seas for the prognosis of hydrologic changes in the estuarine areas of the Ob River and Kara and Pechora seas (in Russian), report, 101 pp., Inst. of Water Stud., Russian Acad. of Sci., Moscow.

Forman, S. L., and L. Polyak (1997), Radiocarbon content of pre-bomb marine mollusks and variations in the ^{14}C reservoir age for coastal areas of the Barents and Kara seas, Russia, *Geophys. Res. Lett.*, *24*, 885–888.

Forman, S. L., D. J. Lubinski, G. H. Miller, G. G. Matishov, S. Korsun, J. Snyder, F. Herlihy, R. Weihe, and V. Myslivets (1996), Postglacial emergence of western Franz Josef Land, Russia, and retreat of the Barents Sea ice shelf, *Quat. Sci. Rev.*, *15*, 77–90.

Giraudeau, J., M. Cremer, S. Manthé, L. Labeyrie, and G. Bond (2000), Coccolith evidence for instabilities in surface circulation south of Iceland during Holocene times, *Earth Planet. Sci. Lett.*, *179*, 257–268.

Graham, D. W., B. H. Corliss, M. L. Bender, and L. D. Keigwin (1981), Carbon and oxygen isotopic disequilibrium of recent deep sea benthic foraminifera, *Mar. Micropaleontol.*, *6*, 483–497.

Grossman, E. L. (1984), Stable isotope fractionation in live benthic foraminifera from the southern California borderland, *Palaeogeogr. Palaeoclimatol. Palaeoecol.*, *47*, 301–327.

Grossman, E. L. (1987), Stable isotope in modern benthic foraminifera: A study of vital effect, *J. Foraminiferal Res.*, *17*, 48–61.

Hald, M., and R. Aspeli (1997), Rapid climatic shifts of the northern Norwegian Sea during the last deglaciation and the Holocene, *Boreas*, *26*, 15–28.

Hald, M., V. Kolstad, L. Polyak, S. L. Forman, F. A. Herlihy, G. Ivanov, and A. Nescheretov (1999), Late-glacial and Holocene paleoceanography and sedimentary environments in the St. Anna Trough, Eurasian Arctic Ocean margin, *Palaeogeogr. Palaeoclimatol. Palaeoecol.*, *146*, 229–249.

Hald, M., K. Husum, T. O. Vorren, K. Grosfjeld, H. B. Jenssen, and A. Sharapova (2003), Holocene climate in the subarctic fjord Malangen, northern Norway: A multiproxy study, *Boreas*, *32*, 543–559.

Hald, M., H. Ebbesen, M. Forwick, F. Godtliebsen, L. Khomenko, S. Korsun, L. R. Olsen, and T. O. Vorren (2004), Holocene paleoceanography and glacial history of the West Spitzbergen area, Euro Arctic margin, *Quat. Sci. Rev.*, *23*, 2075–2088.

Ivanova, E. V., I. O. Murdmaa, J. C. Duplessy, and M. Paterne (2002), Late Weichselian to Holocene paleoenvironments in the Barents Sea, *Global Planet. Change*, *34*, 209–218.

Keigwin, L. D. (1996), The Little Ice Age and Medieval warm period in the Sargasso Sea, *Science*, *274*, 1504–1508.

Keigwin, L. D., and E. A. Boyle (2000), Detecting Holocene changes in thermohaline circulation, *Proc. Natl. Acad. Sci. U. S. A.*, *97*, 1343–1346.

Koç, N., E. Jansen, and H. Haflidason (1993), Paleoceanographic reconstructions of surface ocean conditions in the Greenland, Iceland and Norwegian seas through the last 14 ka based on diatoms, *Quat. Sci. Rev.*, *12*, 115–140.

Labeyrie, L. D., J. C. Duplessy, and P. L. Blanc (1987), Variations in mode of formation and temperature of oceanic deep waters over the past 125,000 years, *Nature*, *327*, 477–482.

Labeyrie, L., et al. (1995), Surface and deep hydrology of the northern Atlantic Ocean during the last 150,000 years, *Philos. Trans. R. Soc. London*, *348*, 255–264.

Lambeck, K., and J. Chappell (2001), Sea level change through the last glacial cycle, *Science*, *292*, 679–686.

Létolle, R., J. M. Martin, A. J. Thomas, V. V. Gordeev, S. Gusarova, and I. S. Sidorov (1993), Oxygen-18 abundance and dissolved silicate in the Lena delta and Laptev Sea (Russia), *Mar. Chem.*, *43*, 47–64.

Levitan, M. A., N. A. Belyaev, M. V. Burtman, J. C. Duplessy, and T. A. Khusid (2003), Holocene sedimentation history in the Southern Novaya Zemlya Trench, *Lithology Miner. Resour.*, *6*, 660–672.

Loeng, H. (1991), Features of the physical oceanographic conditions of the Barents Sea, in *Proceedings of the Pro Mare Symposium on Polar Marine Ecology*, edited by E. Sakshaug, C. C. E. Hopkins, and N. A. Oristland, pp. 5–18, Polar Res., Trondheim, Norway.

Lubinski, D. J., L. Polyak, and S. L. Forman (2001), Freshwater and Atlantic water inflows to the deep northern Barents and Kara seas since ca 13 ^{14}C ka: Foraminifera and stable isotopes, *Quat. Sci. Rev.*, *20*, 1851–1879.

Marchal, O., et al. (2002), Apparent long-term cooling of the sea surface in the northeastern Atlantic and the Mediterranean during the Holocene, *Quat. Sci. Rev.*, *21*, 455–483.

Midttun, L. (1985), Formation of dense bottom water in the Barents Sea, *Deep Sea Res., Part A*, *32*, 1233–1241.

Murdmaa, I. O., and E. Ivanova (1999), Postglacial sedimentation history in the shelf depressions of the Barents Sea (in Russian), *Lithol. Miner. Resour.*, *34*, Engl. Transl., 576–595.

Ostermann, D. R., and W. B. Curry (2000), Calibration of stable isotopic data: An enriched $\delta^{18}O$ standard used for source gas mixing detection and correction, *Paleoceanography*, *15*, 353–360.

Ostlund, H. G., and C. Grall (1993), Arctic tritium, 1973–1991, *Data Rep. 19*, Rosenstiel Sch. of Mar. and Atmos. Sci., Univ. of Miami, Miami, Fla.

Pfirman, S. L., D. Bauch, and T. Gammelsrod (1994), The northern Barents Sea: Water mass distribution and modification, in *The Polar Oceans and Their Role in Shaping the Global Environment*, *Geophys. Monogr. Ser.*, vol. 85, edited by O. Johannessen, R. D. Muench, and J. E. Overland, pp. 77–94, AGU, Washington D. C.

Rimbu, N., G. Lohmann, J. H. Kim, H. W. Arz, and R. Schneider (2003), Arctic/North Atlantic Oscillation signature in Holocene sea surface temperature trends as obtained from alkenone data, *Geophys. Res. Lett.*, *30*(6), 1280, doi:10.1029/2002GL016570.

Risebrobakken, B., E. Jansen, C. Anderson, E. Mjelde, and K. Hevroy (2003), A high-resolution study of Holocene paleoclimatic and paleoceanographic changes in the Nordic Seas, *Paleoceanography*, *18*(1), 1017, doi:10.1029/2002PA000764.

Rudels, B., E. P. Jones, L. G. Anderson, and G. Kattner (1994), On the intermediate depth waters of the Arctic Ocean, in *The Polar Oceans and Their Role in Shaping the Global Environment*, *Geophys. Monogr. Ser.*, vol. 85, edited by O. Johannessen, R. D. Muench, and J. E. Overland, pp. 33–46, AGU, Washington D. C.

Sarnthein, M., S. Van Kreveld, H. Erlenkeuser, P. M. Grootes, M. Kucera, U. Pflaumann, and M. Schulz (2003), Centennial-to-millennial-scale periodicities of Holocene climate and sediment injections off the western Barents shelf, 75°N, *Boreas*, *32*, 447–461.

Schauer, U., H. Loeng, B. Rudels, V. K. Ozhigin, and W. Dieck (2002), Atlantic Water flow through the Barents and Kara Seas, *Deep Sea Res., Part I*, *49*, 2281–2298.

Stuiver, M., and P. J. Reimer (1993), Extended ^{14}C data base and revised CALIB 3.0 ^{14}C age calibration program, *Radiocarbon*, *35*, 215–230.

Vincent, E., J. S. Killingley, and W. H. Berger (1981), Stable isotope composition of benthic foraminifera from the equatorial Pacific, *Nature*, *289*, 639–643.

Waelbroeck, C., L. Labeyrie, E. Michel, J. C. Duplessy, J. F. McManus, K. Lambeck, E. Balbon, and M. Labracherie (2002), Sea-level and deep water temperature changes derived from benthic foraminifera isotopic records, *Quat. Sci. Rev.*, *21*, 295–305.

Woodruff, F., S. S. Savin, and R. G. Douglas (1980), Biological fractionation of oxygen and carbon isotopes by recent benthic foraminifera, *Mar. Micropaleontol.*, *5*, 3–11.

E. Cortijo, J. C. Duplessy, L. Labeyrie, and M. Paterne, Laboratoire des Sciences du Climat et de l'Environnement, Laboratoire mixte CNRS-CEA, Parc du CNRS, 91198 Gif sur Yvette Cedex, France. (jean-claude.duplessy@lsce.cnrs-gif.fr)

E. Ivanova, T. Khusid, and I. Murdmaa, Shirshov Institute of Oceanology, Russian Academy of Sciences, 36 Nakhimonovsky Prospect, 117997 Moscow, Russia.

M. Levitan, Vernadsky Institute of Geochemistry and Analytical Chemistry, Russian Academy of Sciences, ul. Kosygina 19, 119991 Moscow, Russia.

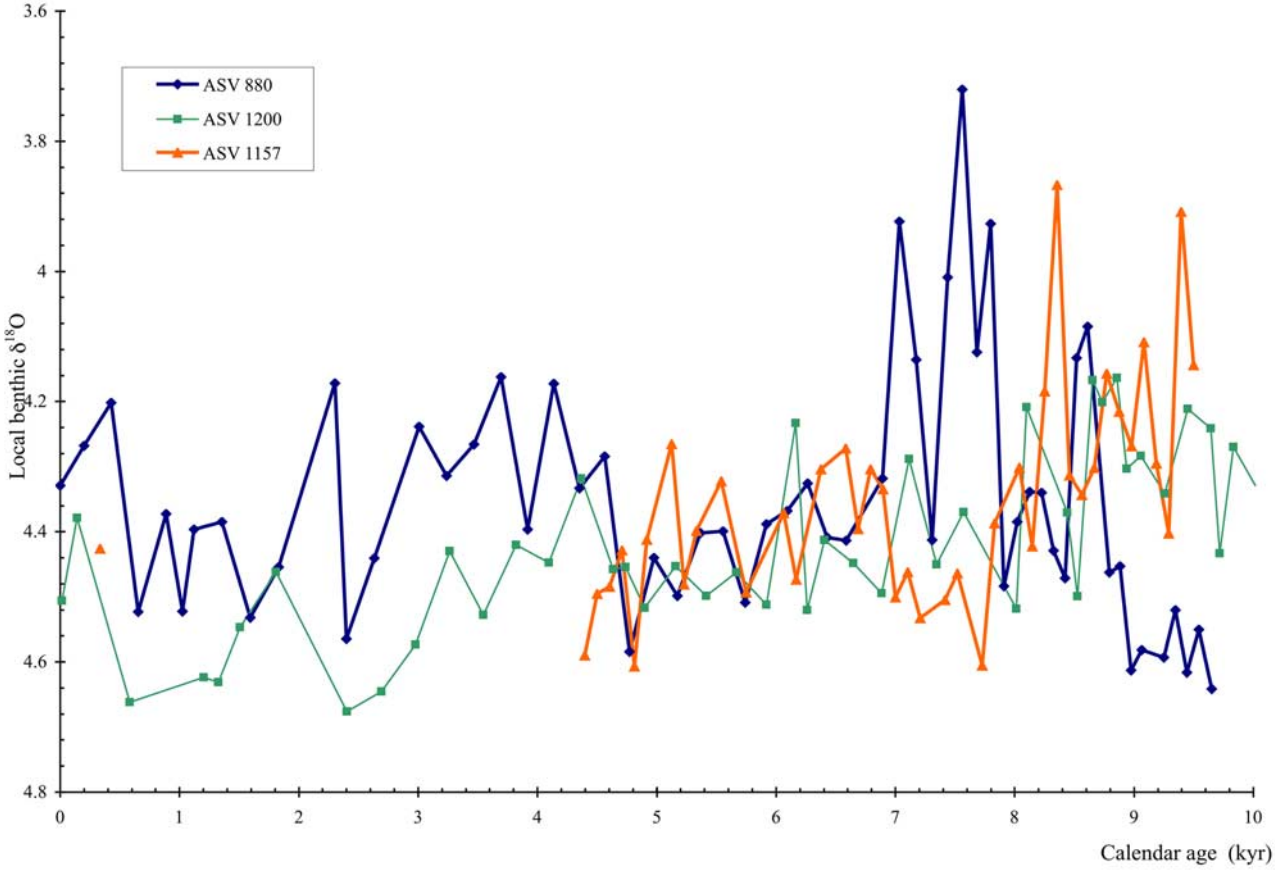

Figure 6. Local oxygen isotope records for benthic foraminifers in cores ASV 880, ASV 1157, and ASV 1200.